RZ 2844 (# 90147) 07/15/96
Physical Sciences 6 pages

Research Report

Near-Field Optical Microscopy: Imaging beyond the Diffraction Limit

D. W. Pohl

IBM Research Division
Zurich Research Laboratory
8803 Rüschlikon
Switzerland

Near-Field Optical Microscopy: Imaging beyond the Diffraction Limit

D. W. Pohl

IBM Research Division, Zurich Research Laboratory, 8803 Rüschlikon, Switzerland

Abstract

The wealth of optical phenomena offers many opportunities for the investigation of individual nanometer-sized structures *if, and only if,* the relevant radiation can be confined to a sufficiently small extension. This can be achieved with material structures having nanometer-sized dimensions themselves. Small apertures, small particles and pointed tips are particularly suited for this purpose. When integrated appropriately into a scanning probe microscope, they provide optical scan images with resolution in the 10 to 100 nm regime. The most successful near-field optical (NFO) microscope to date is the *aperture scanning NFO microscope* (SNOM): It can be operated in transmission or reflection mode, with amplitude, phase and polarization contrast. Its most intriguing mode of operation, however, is fluorescence microscopy, of utmost importance for biological and medical applications. In practical work with SNOM, various types of artifacts have to be avoided that can mask the true near-field images to a large extent. The theoretical description of the imaging process requires the numerical solution of Maxwell's equations for complicated boundary conditions, a (computer-)time consuming but rewarding task.

I. INTRODUCTION

Scanning near-field optical microscopy (SNOM) recently became a focus for scientific and technical interest because it is the only scanning probe microscopy with well understood material specificity (color, polarization, fluorescence). The field is expanding rapidly and hence cannot be covered exhaustively in the space of this short article. For recent reviews, the reader is referred to Refs. [1–4].

II. APERTURE SNOM (a–SNOM)

The most popular SNOM to date is the *aperture (a-)* SNOM (also called NSOM) [5–8]. It is based on a design we developed at IBM ten years ago [5]. Its essential parts are a pointed transparent tip coated with an opaque metal film such that a small aperture is formed at the apex, see Figs. 1a–1c. In the early days, these tips were etched quartz crystals [5,6] or micropipettes [7,8]; nowadays, the tips of choice are optical fibers pulled or etched to a sharp tip at one end [2]. Transparent micromechanical cantilever tips, introduced recently as SNOM probes [9,10], represent a promising new alternative.

The metallic, conical screen that guides the light to the aperture acts as a waveguide that is overdamped near the apex; its transmission decreases heavily with shrinking aperture diameter [11,12]. Therefore, a-SNOM is limited to aperture diameters of about 30 to 70 nm, which provide a resolution of approximately the same size. Waveguide geometries without cutoff, such as coaxial cones or slotted-wall structures [13], might provide larger transmission and allow the resolution to be further improved.

a-SNOMs are usually operated in the "emission mode" (Fig. 1a), meaning that light is focused into the optical probe from the far end. A tiny amount of the radiation is transmitted by the aperture, interacts with the object structure next to it, and is collected by the focusing optics, for instance an auxiliary conventional optical microscope. The "reflection mode" (Fig. 1c), first demonstrated in 1988 [14], has recently been gaining increasing attention [15–18].

To control the gap width between probe and object and to distinguish between topographic and optical features, it is convenient to install an auxiliary distance-sensing mechanism, in

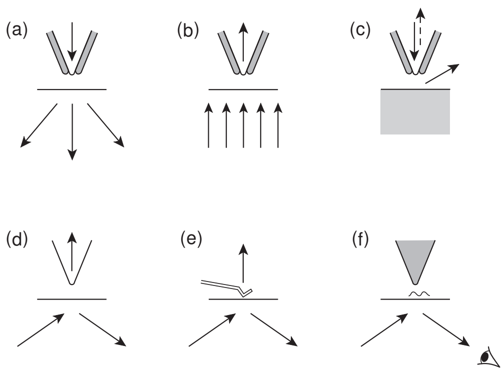

FIG. 1. Various types of NFO probes. Arrows indicate the flow of light. The horizontal line marks the top surface of the object. The optical probe comes from above, and opaque parts are shown shaded. (a)–(c): Aperture probes operated in emission, collection and external reflection mode, respectively. (d)–(f): "Photon scanning tunneling" (PSTM) schemes with fiber, AFM and STM tip, respectively. Reprinted from [4]. Copyright 1994 Springer-Verlag.

general one that monitors the onset of electrical [5,6,8] or mechanical contact (shear [2,19] or normal [9,10] force).

III. “TUNNEL” NEAR-FIELD OPTICAL MICROSCOPE (TNOM)

The tunnel near-field optical microscope (TNOM), see Fig. 2 [20,21], employs a normal aperture tip but detects the light coupled via evanescent waves (photon tunneling) into the object, in addition to the forward-transmitted light (i.e. the regular, “allowed” a-SNOM mode). The “forbidden” contributions are transmitted at angles larger than the critical one and therefore are invisible in a standard a-SNOM. The gap-width–dependent transmission, in general, provides enhanced contrast and is also suitable for distance regulation.

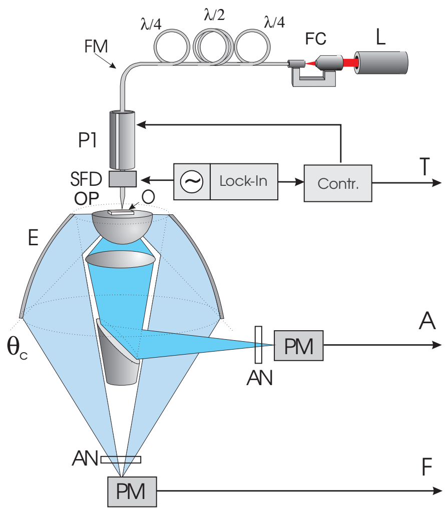

FIG. 2. (a) TNOM setup. L: laser, $\lambda/2$–$\lambda/4$: combination of $\lambda/2$ and $\lambda/4$ plates for polarization adjustment, FC: fiber coupler, FM: monomode fiber with pointed end acting as optical probe (OP); P1: piezoactuator; SFD: shear force detector; E: elliptical mirror; θ_c: critical angle; O: object; AN: polarization analyzers; PM: photomultipliers detecting allowed (A) and forbidden (F) light. Channel T provides the topographic signal derived from the frictional (shear) force interaction. Reprinted from [21] by permission of Kluwer Academic Publishers.

Figures 3 and 4 show some recent TNOM pictures as examples of near-field optical imaging. The individual images represent the simultaneous records of (a) forbidden and (b) allowed light, (c) the topography and (d) the superposition of (a) and (c). Figure 3 shows red blood cells with their characteristic ellipsoidal shape. The optical images reveal various details that are smaller than 100 nm and invisible in the recorded topography. Many features appear with reversed contrast in forbidden and allowed light, which is typical for transparent (phase) objects and allows us to distinguish them from amplitude objects.

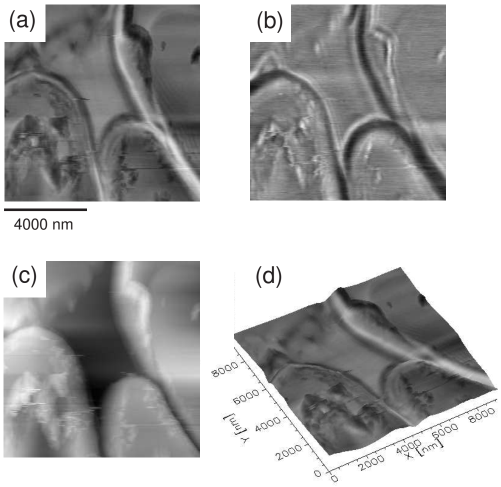

FIG. 3. Red blood cells on a glass substrate, air-dried, and observed with green light: (a) "forbidden", (b) "allowed" light, (c) topography (friction image), and (d) superposition of (a) and (c). Reprinted from [21] by permission of Kluwer Academic Publishers.

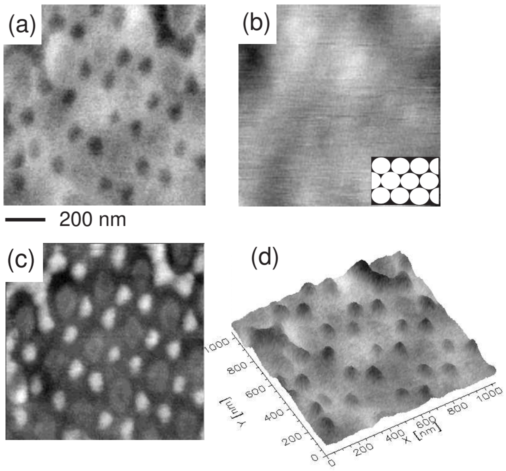

FIG. 4. Glass plate with metallic pattern (Al, thickness 15 nm, lateral extension approximately 50 nm, prepared by U. Ch. Fischer, University of Münster, Germany), image B. Hecht, IBM Rüschlikon. (a) "Forbidden", (b) "allowed" light, (c) topography (friction image), and (d) superposition of (a) and (c). Reprinted from [21] by permission of Kluwer Academic Publishers.

Figure 4 shows TNOM and friction/topographic images of a metal island film as an example of an amplitude object. Moreover, the pictures also demonstrate the immunity of forbidden-light imaging to a background of stray light. The film was structured into triangular patches of about 50 nm diameter by means of the latex-sphere shadowing method [22]. The metal islands (Al, thickness 15 nm) show up as a dark regular pattern in Fig. 4a. Some patches have triangular shape, indicating that the resolution exceeds 50 nm. The allowed image, Fig. 4b, is fairly obscured owing to stray light from imperfections at the sidewall of the optical probe, a shortcoming that sometimes results from the production of optical probe tips. For comparison, in a conventional optical microscope, no structures could be resolved.

IV. SINGLE-MOLECULE SPECTROSCOPY AND OTHER APPLICATIONS

One of the most intriguing capabilities offered by SNOM is the spectroscopy of individual molecules [23–27]. The TNOM geometry is well suited for this purpose, if the detectors shown in Fig. 2 are replaced by an elliptical or a paraboidal mirror, which allows a large portion of the total fluorescence intensity to be collected. The breakup of an inhomogeneous excitation spectrum into contributions from individual molecules, for instance, allows the identification of molecules by their saturation behavior and strong Stark shift (Fig. 5) [26]. Another possible application is, for example, magnetic-domain imaging on the basis of the magneto-optic Kerr effect [28,29].

Major applications may be expected in biological research, as fluorescent labels can be better localized by using SNOM, and in microelectronics, where optical information gained from SNOM will help characterize the materials that form or perturb the surface of electronic circuitry [30–33].

V. THEORETICAL ASPECTS

The ability to separate source, zone of interaction and detector allows different modes of SNOM operation, but also complicates the understanding of near-field phenomena. Near and

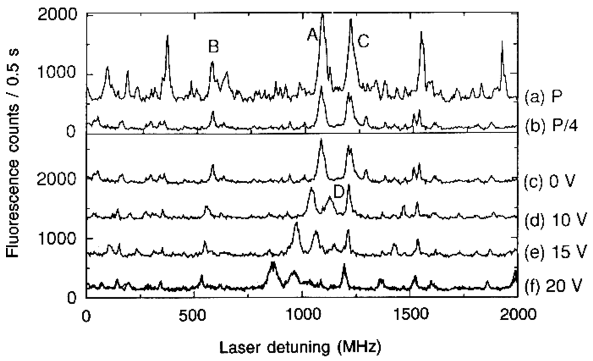

FIG. 5. Statistical fine structure and single-molecule features in the excitation spectrum of a pentacene-doped *p*-terphenyl sample. Upper panel: Spectra taken with (a) 100-μW and (b) 25-μW pump laser power indicate beginning saturation of some absorption lines. Lower panel: Voltage applied to the metallic coating of the optical probe tip causes Stark shift of some lines. Reprinted from [26].

far-field effects have to be considered simultaneously, a problem that cannot be handled by the theoretical tools of classical optics or of electro-statics. As a consequence, the questions of achievable resolution and contrast have mainly been left to heuristic arguments and experimental evidence so far.

The modeling of light propagation through the complicated SNOM geometry requires the numerical solution of Maxwell's equations. It is therefore difficult to arrive at general descriptions of the relevant fields; however, a number of specific configurations have recently been studied [34–39], initiated by a pioneering investigation at the University of Namur [34]. An example is given in Fig. 6, which shows the calculated electrical energy density (squared electric field) for an uncoated, prism-like tip. It can clearly be seen how the evanescent field surrounds the corner of the prism and how it is locally deformed upon approach of a glass substrate.

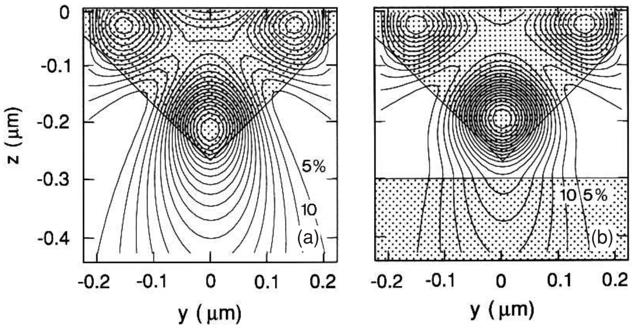

FIG. 6. 2-D modeling of a SNOM tip: energy density in and next to a glass prism illuminated from top, s-polarization. (a) in free space, (b) next to a glass substrate. Reprinted from [34] by permission of Kluwer Academic Publishers.

VI. IN SUMMARY ...

... SNOM is more complex than other scanning probe techniques, but it can also provide a larger variety of information. a-SNOM with ≈ 50 nm resolution has reached a fair level of maturity. To achieve ultimate resolution, possibly in the 1–3 nm regime, it may be necessary to invent new near-field optical probes differing considerably from those used so far.

[1] D. W. Pohl, in *Scanning Tunneling Microscopy II*, Vol. 28 of *Springer Series in Surface Science*, edited by R. Wiesendanger and H.-J. Güntherodt (Springer Verlag, Berlin Heidelberg, 1992), pp. 233–271.

[2] E. Betzig and J. Trautman, Science **257**, 189 (1992).

[3] N. F. van Hulst, M. H. P. Moers, and B. Bölger, J. Microsc. **171**, 95 (1993).

[4] H. Heinzelmann and D. W. Pohl, Appl. Phys. A **59**, 89 (1994).

[5] D. W. Pohl, W. Denk, and M. Lanz, Appl. Phys. Lett. **44**, 651 (1984).

[6] U. Dürig, D. W. Pohl, and F. Rohner, J. Appl. Phys. **59**, 3318 (1986).

[7] A. Harootunian, E. Betzig, M. Isaacson, and A. Lewis, Appl. Phys. Lett. **49**, 674 (1986).
[8] E. Betzig, M. Isaacson, and A. Lewis, Appl. Phys. Lett. **51**, 2088 (1987).
[9] N. F. van Hulst *et al.*, Appl. Phys. Lett. **62**, 461 (1993).
[10] F. Baida, D. Courjon, and G. Tribillon, in *Near Field Optics*, Vol. 242 of *NATO ASI Series E: Applied Sciences*, edited by D. W. Pohl and D. Courjon (Kluwer Academic Publishers, Dordrecht, The Netherlands, 1993), pp. 71–78.
[11] L. Novotny and D. W. Pohl, in *Photons and Local Probes*, Vol. 300 of *NATO ASI Series E: Applied Sciences*, edited by O. Marti and R. Möller (Kluwer Academic Publishers, Dordrecht, The Netherlands, 1995), pp. 21–33.
[12] L. Novotny, D. W. Pohl, and B. Hecht, Opt. Lett. **20**, 970 (1995).
[13] U. C. Fischer and M. Zapletal, Ultramicroscopy **42-44**, 393 (1992).
[14] U. C. Fischer, U. T. Dürig, and D. W. Pohl, Appl. Phys. Lett. **52**, 249 (1988).
[15] J. A. Cline, H. Barshatzky, and M. Isaacson, Ultramicroscopy **38**, 299 (1991).
[16] M. Spajer *et al.*, J. Phys. III **1**, 1 (1991).
[17] S. Jiang, K. Nakagawa, and M. Ohtsu, Jpn. J. Appl. Phys. **33**, L55 (1994).
[18] C. Durkan and I. Shvets, in *Photons and Local Probes*, Vol. 300 of *NATO ASI Series E: Applied Sciences*, edited by O. Marti and R. Möller (Kluwer Academic Publishers, Dordrecht, The Netherlands, 1995), pp. 145–150.
[19] R. Toledo-Crow, P. C. Yang, Y. Chen, and M. Vaez-Iravani, Appl. Phys. Lett. **60**, 2957 (1992).
[20] B. Hecht, H. Heinzelmann, and D. Pohl, Ultramicroscopy **57**, 228 (1995).
[21] B. Hecht, D. W. Pohl, H. Heinzelmann, and L. Novotny, in *Photons and Local Probes*, Vol. 300 of *NATO ASI Series E: Applied Sciences*, edited by O. Marti and R. Möller (Kluwer Academic Publishers, Dordrecht, The Netherlands, 1995), pp. 93–107.
[22] U. C. Fischer and H. P. Zingsheim, J. Vac. Sci. Technol. **19**, 881 (1981).
[23] J. K. Trautman, J. J. Macklin, L. E. Bruns, and E. Betzig, Nature **369**, 40 (1994).
[24] X. S. Xie and R. C. Dunn, Science **265**, 361 (1994).
[25] W. P. Ambrose, P. M. Goodwin, J. C. Martin, and R. A. Keller, Science **265**, 364 (1994).
[26] W. E. Moerner *et al.*, Phys. Rev. Lett. **73**, 2764 (1994).
[27] A. J. Meixner, D. Zeisel, M. A. Bopp, and G. Tarrach, Opt. Engin. **34**, 2324 (1995).
[28] E. Betzig *et al.*, Appl. Phys. Lett. **61**, 142 (1992).
[29] T. J. Silva, S. Schultz, and D. Weller, Appl. Phys. Lett. **65**, 658 (1994).
[30] R. Dunn, G. Holtom, L. Mets, and X. Xie, J. Phys. C **98**, 3094 (1994).
[31] E. Betzig, R. J. Chichester, F. Lanni, and D. L. Taylor, Bioimaging **1**, 129 (1994).
[32] M. H. P. Moers, H. E. Gaub, and N. van Hulst, Langmuir **10**, 2774 (1994).
[33] N. F. van Hulst, M. H. P. Moers, and E. Borgonjen, in *Photons and Local Probes*, Vol. 300 of *NATO ASI Series E: Applied Sciences*, edited by O. Marti and R. Möller (Kluwer Academic Publishers, Dordrecht, The Netherlands, 1995), pp. 165–180.
[34] A. Dereux and D. Pohl, in *Near Field Optics*, Vol. 242 of *NATO ASI Series E: Applied Sciences*, edited by D. W. Pohl and D. Courjon (Kluwer Academic Publishers, Dordrecht, The Netherlands, 1993), pp. 189–198.
[35] L. Novotny, D. W. Pohl, and P. Regli, J. Opt. Soc. Am. A **11**, 1768 (1994).
[36] N. Garcia and M. Nieto-Vesperinas, Theory of the Apertureless Near-Field Optical Microscope: Image Resolution, (Preprint).
[37] C. Girard and A. Dereux, Phys. Rev. B **49**, 11344 (1994).
[38] O. J. F. Martin, C. Girard, and A. Dereux, Phys. Rev. Lett. **74**, 526 (1995).
[39] D. V. Labeke and D. Barchiesi, J. Opt. Soc. Am. A **9**, 732 (1992).